Available online at www.sciencedirect.com
SCIENCE DIRECT®
Journal of Nuclear Materials 344 (2005) 191–197
journal of nuclear materials
www.elsevier.com/locate/jnucmat

A thermodynamic approach for advanced fuels of gas-cooled reactors

C. Guéneau [a,*], S. Chatain [a], S. Gossé [a], C. Rado [b], O. Rapaud [b], J. Lechelle [c], J.C. Dumas [d], C. Chatillon [e]

[a] *DEN/DPC/SCP – CEA Saclay, 91191 Gif-sur-Yvette cedex, France*
[b] *DEN/DTEC/STCF – CEA Valrho, 26702 Pierrelatte cedex, France*
[c] *DEN/DEC/SPUA – CEA Cadarache, 13108 Saint-Paul Lez Durance cedex, France*
[d] *DEN/DEC/SESC – CEA Cadarache, 13108 Saint-Paul Lez Durance cedex, France*
[e] *LTPCM – UMR5614, ENSEEG BP75 Grenoble, 38402 Saint-Martin d'Hères cedex, France*

Abstract

For both high temperature reactor (HTR) and gas cooled fast reactor (GFR) systems, the high operating temperature in normal and accidental conditions necessitates the assessment of the thermodynamic data and associated phase diagrams for the complex system constituted of the fuel kernel, the inert materials and the fission products. A classical CALPHAD approach, coupling experiments and thermodynamic calculations, is proposed. Some examples of studies are presented leading with the CO and CO_2 gas formation during the chemical interaction of $[UO_{2\pm x}/C]$ in the HTR particle, and the chemical compatibility of the couples [UN/SiC], [(U, Pu)N/SiC], [(U, Pu)N/TiN] for the GFR system. A project of constitution of a thermodynamic database for advanced fuels of gas-cooled reactors is proposed.
© 2005 Elsevier B.V. All rights reserved.

PACS: 07.75; 64.75.+g; 81.05.Je; 81.05.Uw; 81.30.−t; 82.60.−s

1. Introduction

Within the frame of the Generation IV project, CEA is interested in two types of gas-cooled reactors [1]:

- the high temperature reactor (HTR) whose development is mainly based on the knowledge achieved in the seventies. The current needs are related to a higher operating temperature for the fuel and the structural materials;
- the gas cooled fast reactor (GFR) for electricity production, whose fuel cycle is optimised to recycle actinides and to minimise the waste production. No complete reference system exists. The needs are considerable and concern the choice of the core and structural materials, the passive safety system capabilities and the recycle techniques.

In both cases, the fuel may operate at about 1000–1200 °C in normal conditions and may reach 1600–1700 °C in case of accident.

For the HTR concept, classical TRISO particles are considered (Fig. 1) [2,3]. The fuel kernel, made of pure

* Corresponding author.
E-mail address: cgueneau@cea.fr (C. Guéneau).

0022-3115/$ - see front matter © 2005 Elsevier B.V. All rights reserved.
doi:10.1016/j.jnucmat.2005.04.041

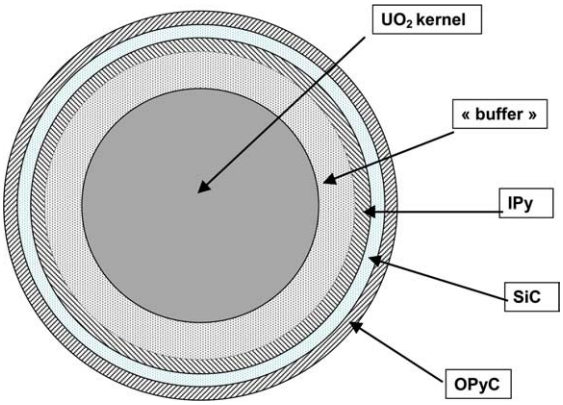

Fig. 1. Schematic view of a TRISO particle.

UO_2 or of a mixture of UO_2 and UC_2, is surrounded by several successive coating layers:

- a graphite buffer layer that accommodates the noble and CO, CO_2 gas release as well as fuel swelling;
- an inner pyrolytic carbon layer that protects the SiC layer from chemical reactions with both fuel and fission products;
- a silicon carbide layer that decreases solid fission product diffusion out of the particle and enhances the mechanical behaviour of the system;
- an outer pyrolytic carbon layer that protects the SiC layer and contributes to the particle mechanical strength; in case of failure of the SiC layer, this layer must play the role of barrier towards fission product diffusion. ZrC is also considered to replace SiC.

For the GFR system, the criteria for the choice of the core materials are the following ones: a high volume fraction of actinide, a geometry and thermal properties that allow a fast cooling, gas temperatures ranging from 400 to 850 °C (1200 °C–1600 °C in accidental conditions), a mechanical strength towards gas pressure and the fission product retention [4]. (U, Pu)C carbides and (U, Pu)N nitrides are candidates for the fuel kernel because of their high actinide density, and their elevated decomposition temperature and thermal conductivity. Several fuel forms are considered: composite ceramic–ceramic fuel (cercer) with closely packed fuel kernels or fibers, advanced fuel particles with large fuel kernels and thin coatings or ceramic clad, solid-solution metal (cermet) fuels.

The choice of the fuel coating materials has to meet some constraints regarding fast neutron damage, mechanical behaviour, thermal properties... but also chemical compatibility with the fuel kernel from 1000 °C to about 2000 °C. The most promising materials for core structures are ceramics such as SiC, ZrC, TiC, TiN, ZrN... that may be inert towards the fuel kernel [4]. In case of a chemical interaction between the fuel kernel and the ceramic, an intermediate layer of a material could be added to play the role of barrier.

2. Needs

For the HTR system, the thermomechanical behaviour of the particle is function of CO, CO_2 and fission product release which gas pressures must be well known to calculate the stresses on the inner pyrolytic carbon, SiC and outer pyrolytic layers as well as of the chemical state of fission products and their diffusion coefficients which influence thermal conductivity, creep and melting point of the fuel [5]. Thermodynamic calculations or empirical laws are commonly used to estimate the CO and CO_2 release in the TRISO particle as a function of UC_2 fraction, enrichment, burnup value and temperature [6]. To better understand and predict CO and CO_2 release in the fuel, a study on the vaporization of CO and CO_2 in the U–C–O system is in progress. The objective is to provide realistic vaporization laws for CO and CO_2 partial pressures in the TRISO particle by determining the deviation from the thermodynamic equilibrium and the role of diffusion in the interfacial reaction between UO_2 fuel and graphite. To take into account the role of fission products on the CO, CO_2 release and to understand, control and predict the chemical interactions in the irradiated fuel particle and the escape of fission products from a defective fuel in normal and accidental conditions, the thermodynamic properties of all gas, liquid and solid phases and the associated phase diagrams of the system [fuel particle with fission products] have to be assessed.

For the GFR system, before considering fission products, the chemical compatibility between the fuel kernel (U, Pu)C or (U, Pu)N and the different considered ceramic matrices (SiC, ZrC, TiC, TiN, ZrN) has first to be studied from 1000 °C to 2000 °C in order to choose the materials for the system [fuel + inert matrix]. In a second step, the chemical state of fission products will be also needed.

For both HTR and GFR systems, a thermodynamic database containing both the constituents of the core materials and the fission products has to be developed.

3. Thermodynamic approach

A usual coupling of experiments and thermodynamic calculations is proposed by using the CALPHAD method. In this method, the Gibbs energy functions of all solid, liquid and gas phases are assessed on the basis of the available experimental data (both phase diagrams and thermodynamic data). The CALPHAD method presents several advantages: it allows to calculate thermodynamic equilibria and associated phase diagrams for

complex materials containing a lot of elements from the extrapolation of binary and ternary sub-systems; it requires a critical analysis of all available experimental thermodynamic data reported in the literature which leads to a consistent set of experimental data; it helps to define the experimental programs necessary to perform as well as to prepare and to interpret new experiments.

For the PWR system, different databases were developed in the past. For example, one was dedicated to the irradiated fuel studies, mainly to determine the chemical state of the fission products and the associated oxygen chemical potential of the fuel [7]. In this case, only stoichiometric compounds were described except the solid solution (U, Pu, fission products)$O_{2\pm x}$ for which a complete assessment of oxygen chemical potential variation with the oxygen stoichiometry (oxygen under metal ratio) and temperature was performed. An other database, NUCLEA, was independently developed by Thermodata to study the physicochemical behaviour of the corium in the framework of severe nuclear accident studies [8]. NUCLEA allows calculating phase diagrams but is only valid at high temperature.

For the gas-cooled reactors, a more suitable solution would be to develop a single database with the fission products valid for both normal and accidental conditions. In both HTR and GFR systems, even if temperatures as high as 3000 °C will not be reached in accidental conditions, the temperature level remains elevated (lower than 2000 °C) and then requires the calculation of phase diagrams. If the list of elements involved in the HTR concept is known, it is not the case for the GFR system. For this one, the oxygen interaction with carbide and nitride fuels has to be considered in case of accident. Therefore, a lot of sub-systems are common to both HTR and GFR fuels. For the GFR system, the priority is to develop a database for the different considered couples [fuel/inert matrix]. At longer term, the objective is to assess the thermodynamic properties of all gas, liquid and solid phases for HTR and GFR advanced gas reactor fuels with the fission products. In a first step, thermodynamic calculations are performed using the existing databases for ternary or quaternary sub-systems, waiting for the development of a single one dedicated to HTR and GFR fuels.

4. Examples

The first example concerns the HTR fuel assembly when the two following ones lead with GFR's system.

4.1. HTR fuel: $UO_{2\pm x}$/C chemical interaction in the TRISO particle

As reported in the previous section, prediction of the thermochemical behaviour of the TRISO particle requires realistic laws of CO and CO_2 release [5]. The purpose of the present work is to use high temperature mass spectrometry to study the kinetic of CO and CO_2 formation from the interaction between $UO_{2\pm x}$ and C in the TRISO particle. In a first step, thermodynamic properties of the U–O–C ternary system are assessed. It requires a critical analysis of literature data. In a second part of the work, the deviation from thermodynamic equilibrium will be determined. The fission products are progressively taken into account by thermodynamic calculations with a database which development is in progress.

4.1.1. Critical analysis of CO partial pressure measurements in U–C–O

Most of CO measurements were performed in three-phase domains of the phase diagram [$UC_2 + UO_2 + C$] [9–16], [$UC_2 + UC_{1-x}O_x + UO_2$] [9,10,15,17,18] and [$U + UC_{1-x}O_x + UO_2$] [9,19]. Some discrepancies exist between available experimental data. As an example, measurements in the [$UC_2 + UO_2 + C$] domain are analysed. In most of the experiments, CO partial pressures in a heated vessel were measured with a gauge placed at a cold point (room temperature). In case of a molecular flow regime (low pressures), when the Knudsen number Kn is lower than 3 (Knudsen number = hole diameter/mean free path of the CO molecule), a correction must be applied that takes into account the thermal effusion effect [20]. This effect leads to a pressure gradient due to the existence of a temperature gradient. By considering that in static conditions, the flux coming from the hot point (heated specimen) is equal to the flux coming from the cold point ($T_0 = 300$ K), the thermal effusion correction is applied as follows:

$$p_{CO}^{corr} = p_{CO}^{300\,K}\sqrt{\frac{T}{300}}. \quad (1)$$

In case of a transition regime ($3 < Kn < 80$), the gas flow is considered as a mix of both molecular and isentropic parts by the following equation [21]:

$$p_{CO}^{corr} = (1-\theta)p_{CO}^{300\,K} + \theta p_{CO}^{300\,K}\sqrt{\frac{T}{300}} \quad (2)$$

with $\theta = 1.05^{-Kn}$, the molecular part of the gas flow. As an example, CO measured and corrected partial pressures are reported in Fig. 2. The corrected pressures correspond to an increase by a factor three. A good agreement is obtained finally between all authors.

4.1.2. Thermodynamic calculations on U–C–O

A database on the ternary system U–C–O is constituted from the U–O, U–C and C–O binary systems which thermodynamic functions are reported in [22–24]. The thermodynamic functions of both $UC_{1\pm x}O_y$ and $UC_{2-x}O_x$ oxycarbides of uranium are evaluated by representing mainly Henry's experimental data [25].

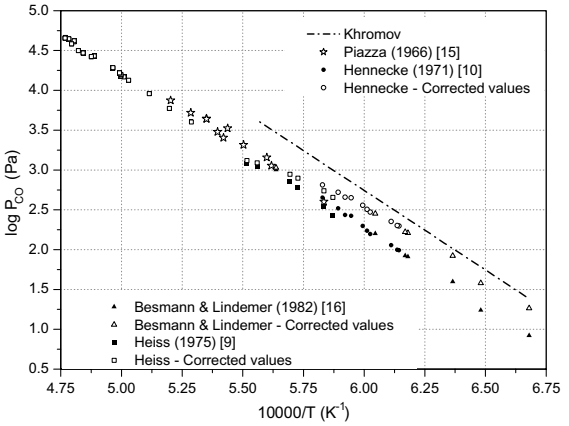

Fig. 2. Experimental and corrected data for CO partial pressures above the three phase domain [$UC_2 + UO_2 + C$].

For $UC_{1\pm x}O_y$, the sublattice model $(C_1,C_2,O, Va)_1(U)_1$ is used. Two interaction parameters between UC and 'UO' and between 'UO' and UC_2, respectively equal to −95 kJ/mol and −38 kJ/mol, are optimized to fit the experimental limit of the $UC_{1\pm x}O_y$ oxycarbide composition domain reported in [25]. For the metastable compound 'UO', the Gibbs energy of formation estimated by Potter is used [26]. By comparison with previous calculations where the monooxycarbide was represented as a solid solution between UC and 'UO', the present model allows to take into account a U/(C + O) ratio that can deviate from 1. As shown in Fig. 3(a) and (b), the calculated composition range of the monooxycarbide is in good agreement with Henry's experimental data [25]. For the dioxycarbide, a similar model $(C_1,C_2,O, Va)_1(U)_1$ is chosen. An ideal solution between UC_2 and UO_2 is considered. A solubility of several percents of oxygen in UC_2 can be obtained when the Gibbs energy of the tetragonal fictive UO_2 is fixed to the one of the cubic UO_2 plus 52 kJ/mol.

The main remaining uncertainties on phase diagram and thermodynamic properties of U–O–C concern the phase diagram at temperatures lower than 1573 K for which no experimental data exist and thermodynamic data for the dioxycarbide of uranium and its associated oxygen solubility limit for which experimental data are scarce and scattered. This lack of experimental data could have important consequences concerning the behaviour of a ($UO_2 + UC_2$) fuel for HTR's system. In normal conditions, at 1273 K, the dicarbide of uranium is not thermodynamically stable (in U–C, the temperature of formation is of about 1750 K). In presence of UO_2, UC_2 dissolves some oxygen and then becomes stabilized. But the temperature of formation of the ternary phase $UC_{2-x}O_x$ in U–O–C is not known.

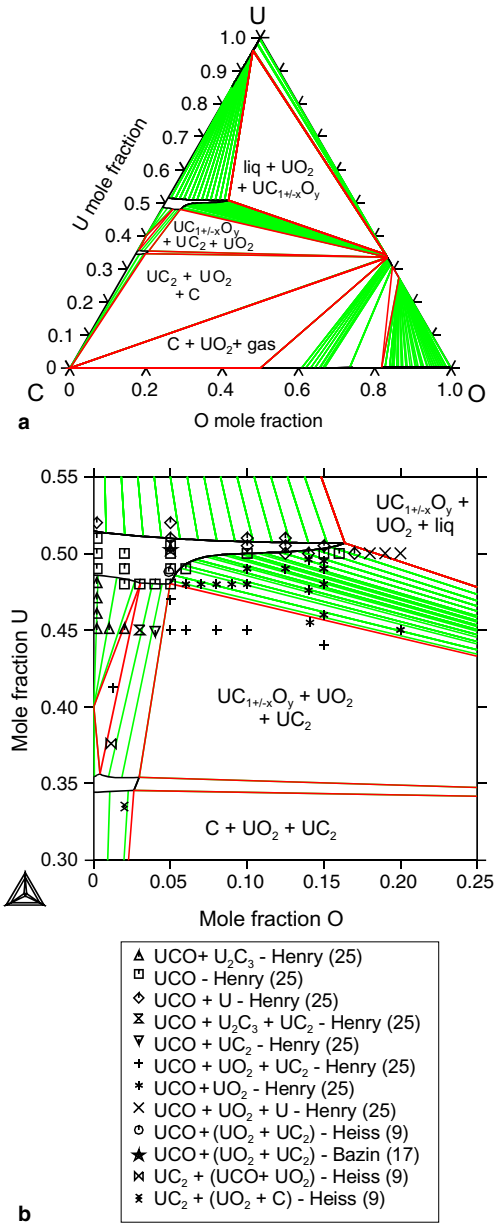

Fig. 3. (a) U–O–C isothermal section calculated at 1973 K where available experimental data are reported. (b) Magnification of the U–O–C isothermal section calculated at 1973 K showing the composition ranges of both uranium oxycarbides. 'UCO' denotes the $UC_{1\pm x}O_y$ oxycarbide.

4.1.3. Equilibrium CO and CO_2 partial pressures during $UO_{2\pm x}$/C interaction

Fig. 4(a) shows the calculated equilibrium partial pressure of CO along the U–CO composition line represented in the U–O–C calculated isothermal section at 1773 K in Fig. 4(b). The CO and CO_2 partial pressures vary very sharply, specially in the two-phase domain

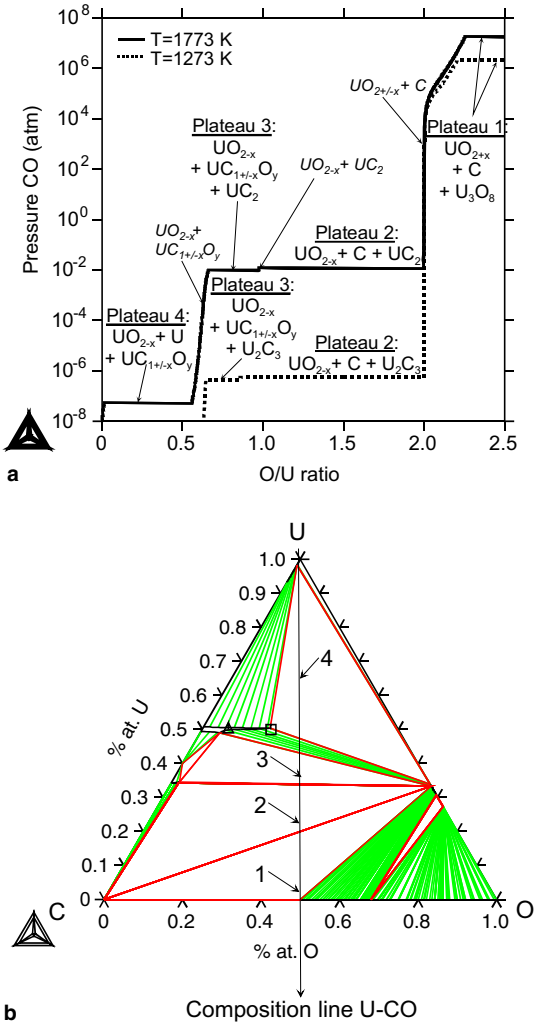

Fig. 4. (a) CO partial pressure variation along the U–CO composition line at 1273 K and 1773 K. (b) U–O–C isothermal section calculated at 1773 K where the U–CO composition line is reported.

$[UO_{2\pm x} + C]$ due to the variation of oxygen potential in the non-stoichiometric compound $UO_{2\pm x}$. In the TRISO particle, a solution to fix the CO partial pressure at a low value consists of adding UC_2 to UO_2.

The present thermodynamic approach may overestimate CO and CO_2 partial pressures. In fact, in the reaction of a gas formation from two solid phases, kinetics associated to diffusion phenomena at the $[UO_2/C]$ interface must play an important role. In the present study, the objective is to determine the kinetic of the CO and CO_2 formation from $UO_{2\pm x}$ and carbon interaction by high temperature mass spectrometry. The present experimental method is used to determine both evaporation (α) and condensation (β) coefficients for CO [27].

4.2. UN/SiC chemical interaction in GFR fuel

In the present work, both thermodynamic properties and associated phase diagrams of the literature are reviewed. Thermodynamic calculations are performed with Gemini 2 code [8] and associated databases, upgraded by using data from the literature. In order to validate isothermal sections or to determine composition of the phases in equilibrium, specific experiments are achieved.

4.2.1. Thermodynamic calculations on U–N–Si–C

In the quaternary system U–N–Si–C, the thermodynamic parameters of Si–C and Si–N binary systems come from Seifert et al. [28]. The Gibb's energy of Si_3N_4 is taken from Hillert et al. [29]. The calculated isothermal sections of the Si–C–N system are in good agreement with generally admitted sections [28]. The Si–U–N system is assessed only from the binary descriptions. A high solubility of Si in UN is reported from a single work in the literature [30]. This surprising behaviour must be verified before taking it into account in the database. The U–C–N ternary system is built from U–C and U–N binary systems. A complete solubility of UC in UN exists, characterized by an interaction parameter λ_{UC-UN}. In order to simplify the calculations, UC and UN are considered as stoichiometric compounds in the temperature range of interest. A critical review of literature's data leads to a value close to zero (ideal solution) for the interaction parameter λ_{UC-UN}.

4.2.2. UN/SiC chemical interaction at 1400 °C under argon gas flow

The chemical interaction is experimentally studied by thermogravimetry (Setaram TG92). The sample is constituted of UN and SiC powders, which are compacted together under 800 MPa. The pellet, placed into an alumina crucible, is heated at 1400 °C during 20 h. An optical micrograph of the sample is presented in Fig. 5 where UN, SiC, and uranium silicide ($USi_{1.88}$) are identified by using WDS analysis (Cameca SX100). The thermodynamic calculations are performed with an argon volume calculated from both argon flow and duration of the experiment. At 1400 °C, the calculation leads at the equilibrium to the following phases: $UC_{0.12}N_{0.88}$, $USi_{1.88}$ and $P(N_2) = 1 \times 10^{-4}$ atm. The agreement between predicted calculations and experimental results is quite good.

4.2.3. UN/SiC chemical interaction in reactor conditions

Between 1000 and 1450 °C, thermodynamic calculations performed for a fuel constituted of a UN kernel with 15% of free volume surrounded by a SiC matrix lead to the formation of UC_xN_{1-x}, Si_3N_4 and USi_3. From about 1450 °C, a liquid phase appears, enriched

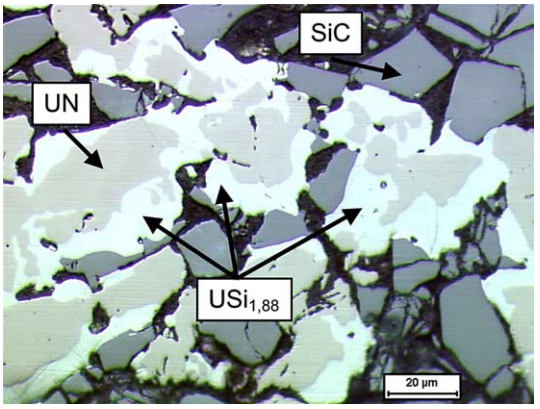

Fig. 5. Optical micrograph of a [UN/SiC] sample heated at 1400 °C during 20 h under argon flow.

in Si (80 at.% Si, 20 at.% U). This phenomenon could cause the damage of the inert matrix. Due to a lack of experimental data on the liquidus, a focussed thermodynamic study on phase equilibria for the U–Si–C ternary system is necessary to determine experimentally the temperature of the liquid formation.

4.3. (U, Pu)N/SiC and (U, Pu)N/TiN chemical interaction in GFR fuel

[$(U_{0.78}Pu_{0.22})$N/SiC] powder coming from the fabrication intended to NIMPHE irradiation experiments is used [31,32]. A first experiment has been carried out with pure polycrystalline SiC (β-SiC) at 1600 °C for 100 h under static argon. XRD analysis of the specimen allows to identify both main initial products and secondary phases such as α-SiC and a compound, denoted MSi_3 (with M:U or/and Pu) that will be further characterized by using an electron microprobe. The electron micrograph in Fig. 6 shows the presence of the actinide

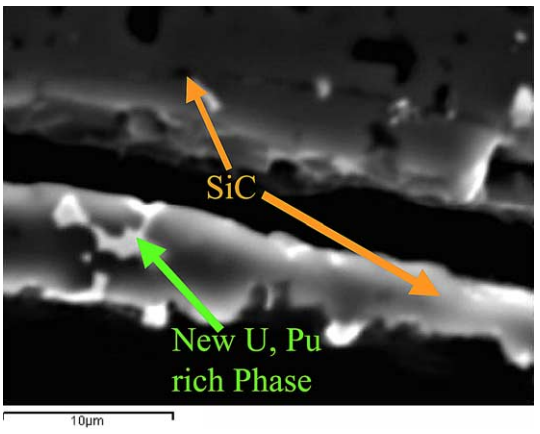

Fig. 6. SEM micrograph of the [$(U_{0.78}Pu_{0.22})$N/SiC] sample heated at 1600 °C for 100 h under static argon.

silicide. Two other experiments are performed with sintered SiC (α-SiC with 1 wt% B_4C) at 1600 °C during 4 h under argon flow and for 100 h under (96.5% Ar + 3.5% N_2). In both cases, the major phases are the actinide compounds (with a possible substitution of N by C) and α-SiC. The secondary phases are B_4C as well as probably MSi_2 (with M:U or/and Pu). On the contrary, for the same heat treatments on [$(U_{0.78}Pu_{0.22})$N/TiN] powder, no secondary phases are present. These first results show that TiN has a lower reactivity towards (U, Pu)N than SiC.

5. Conclusion

For both HTR and GFR systems, the high fuel operating temperature requires the assessment of both thermodynamic data and phase diagrams for the [fuel kernel + inert materials + fission products] system, specially for carbide and nitride fuels. A thermodynamic database associated to a Gibbs energy minimizer code is a necessary tool to help the fabrication process and the fuel design as well as to understand and predict the physico-chemical behaviour of such complex systems in normal and long duration working as well as in accidental conditions.

References

[1] F. Carré, NEA workshop on 'R&D needs for current and future nuclear systems', 6–8 November 2002, Paris.
[2] G.K. Miller, D.A. Petit, D.J. Varacalle, J.T. Maki, J. Nucl. Mater. 317 (2003) 69.
[3] C. Than, Y. Tang, J. Zhu, Y. Zou, J. Li, X. Ni, Nucl. Des. Eng. 218 (2002) 91.
[4] N. Chauvin, in: The 2004 Frédéric Joliot and Otto Hahn Summer School, August 25–September 3, 2004, Cadarache, France.
[5] M. Phelip, G. Degeneve, M. Pelletier, F. Michel, P. Guillermier, The ATLAS HTR Fuel Simulation Code: Objectives, Description and First Results. (AREVA) HTR 2004, Sep. 2004, Pékin (Chine).
[6] A. Petti, T.J. Dolan, G.K. Miller, R.L. Moore, W.K. Terry, A.M. Ougouag, C.H. Oh, H. D. Gougar, Report INEEL/EXT-02-01545, Nov. 2002.
[7] R. Schram, R. Konings, W. Rijinsburger, 'TBASE CONSULT Manual', The Netherlands Energy Research Foundation ECN, updated version of the 05/12/2002.
[8] THERMODATA, 6 rue de l'Eau 38400 Saint-Martin d'Hères, France.
[9] A. Heiss, J. Nucl. Mater. 55 (1) (1975) 207.
[10] J.F.A. Hennecke, H.L. Scherff, J. Nucl. Mater. 38 (1971) 285.
[11] R. Ainsley, B.R. Harder, N. Hodge, R.G. Sowden, D.B. White, D.C. Wood, UKAEA report, AERE-R 4327, 1963.
[12] A.D. Butherus, R.B. Leonard, G.L. Buchel, H.A. Eick, Inorg. Chem. 5 (9) (1966) 1567.

[13] R. Lorenz, H.L. Scherff, N. Toussaint, J. Inorg. Chem. 31 (1969) 2381.
[14] Y.F. Khromov, R.A. Lyutikov, At. Energ. 49 (1) (1980) 28.
[15] J.R. Piazza, M.J. Sinnott, J. Chem. Eng. Data 7 (1962) 451.
[16] T.M. Besmann, T.B. Lindemer, J. Chem. Thermodyn. 14 (3) (1982) 419.
[17] J. Bazin, A. Accary, Bull. Soc. Franç. Ceram. (77) (1967) 109.
[18] T.M. Besmann, J. Am. Soc. 66 (5) (1983) 353.
[19] R.F. Stoops, J.V. Hamme, J. Am. Ceram. Soc. 47 (1964) 59.
[20] S. Dushman, Scientific foundations of vacuum technique, 2nd Ed., John Wiley and Sons, New York, 1966.
[21] S.F. DeMuth, J.S. Watson, J. Vac. Sci. Technol. A 4 (3) (1986).
[22] C. Guéneau, M. Baichi, D. Labroche, C. Chatillon, B. Sundman, J. Nucl. Mater. 304 (2002) 161.
[23] P.Y. Chevalier, E. Fischer, B. Cheynet, J. Nucl. Mater. 288 (2001) 100.
[24] I. Ansara, B. Sundman, Scientific group thermodata Europe, in: P.S. Glaser (Ed.), Computer handling and determination of data, North Holland, Amsterdam, 1986, p. 154.
[25] J.L. Henry, D.L. Paulson, R. Blickensderfer, H.J. Kelly, US Bureau of Mines Report 6968, 1967.
[26] P.E. Potter, J. Nucl. Mater. 42 (1) (1972) 1.
[27] M. Heyrman, C. Chatillon, Electrochem. Soc. Proc. 2003-16 (2003) 503.
[28] H.J. Seifert, J. Peng, H.L. Lukas, F. Aldinger, J. Alloys Compd. 320 (2001) 251.
[29] M. Hillert, S. Jonsson, B. Sundman, Z. Metallkd. 83 (9) (1992) 648.
[30] S. Imoto, K. Niihara, H.J. Stöcker, in: Proceedings of the Symposium on Thermodynamics of Nuclear Materials, IAEA, Vienna, 371, 1968.
[31] H. Bernard, J. Nucl. Mater. 166 (1–2) (1989) 105.
[32] H. Bernard, P. Bardelle, D. Warin, IAEA Technical Committee Meeting on Advanced Fuel for FBR, 3–5 November 1987, Vienne.